Accepted Manuscript

Discovery of potent, orally bioavailable ERK1/2 inhibitors with isoindolin-1-one structure by structure-based drug design

Dezhong Ji, Lingzhi Zhang, Qihua Zhu, Ying Bai, Yaoyao Wu, Yungen Xu

PII: S0223-5234(18)31077-8

DOI: https://doi.org/10.1016/j.ejmech.2018.12.040

Reference: EJMECH 10973

To appear in: *European Journal of Medicinal Chemistry*

Received Date: 10 October 2018

Revised Date: 28 November 2018

Accepted Date: 16 December 2018

Please cite this article as: D. Ji, L. Zhang, Q. Zhu, Y. Bai, Y. Wu, Y. Xu, Discovery of potent, orally bioavailable ERK1/2 inhibitors with isoindolin-1-one structure by structure-based drug design, *European Journal of Medicinal Chemistry* (2019), doi: https://doi.org/10.1016/j.ejmech.2018.12.040.

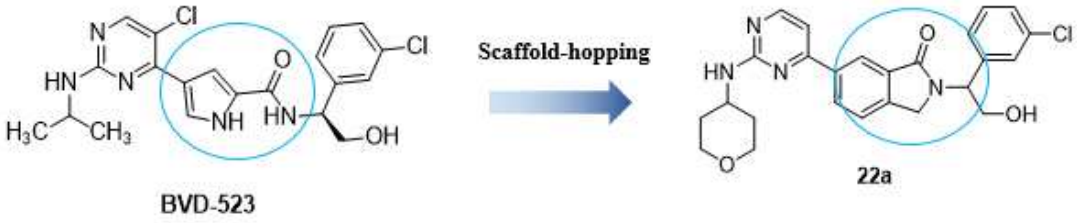

BVD-523

22a

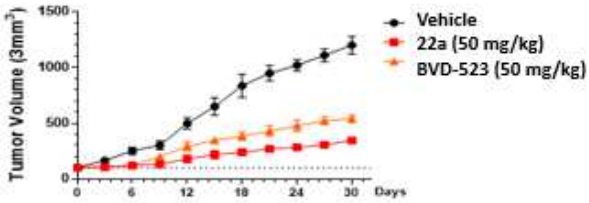

HCT-116 mouse xenograft model

Discovery of potent, orally bioavailable ERK1/2 inhibitors with isoindolin-1-one structure by structure-based drug design

Dezhong Ji[a, £], Lingzhi Zhang[b, £], Qihua Zhu*[, a, b], Ying Bai[b], Yaoyao Wu[b], Yungen Xu*[, a, b]

[a] Jiangsu Key Laboratory of Drug Design and Optimization, China Pharmaceutical University, Nanjing, 21009, China

[b] Department of Medicinal Chemistry, China Pharmaceutical University, Nanjing, 210009, China

[£] Both authors contributed equally to this work

ABSTRACT

Constitutive activation of MAPK (RAS/RAF/MEK/ERK) pathway is frequently observed in many tumors and thus has become an interesting therapeutic target for cancer therapy. Despite the successful development of BRAF and MEK inhibitors in clinic treatment, resistance often appears to re-enhance ERK1/2 signaling. Inspired by the central role of the ERK1/2 signaling cascade in cancer, we describe the scaffold-hopping generation of a series of isoindolin-1-one ERK1/2 inhibitors. Our new compounds could inhibit proliferation of KRAS and BRAF mutant cells lines at low nanomolar concentrations. Compound 22a possesses acceptable pharmacokinetic profiles and showed considerable in vivo antitumor efficacy in a HCT-116 xenograft model, providing a promising basis for further optimization towards clinical ERK1/2 inhibitors.

1. INDTODUCTION

The extracellular signal-regulated kinase (ERK) mitogen-activated protein kinase (MAPK) pathway plays a central role in controlling mammalian cellular functions, including adhesion, migration, differentiation, metabolism, and proliferation.[1] This pathway is activated by a variety of extracellular stimulus, resulted in activation of the RAS (KRAS, NRAS, and HRAS) and then leads to the recruitment and activation of RAF, a serine-threonine kinase. Subsequently, signal is transmitted downstream through activated RAF by activates its main substrates MEK1 and MEK2, which are dual-specificity kinases that activate their only substrates ERK1 and ERK2 via the phosphorylation of conserved threonine and tyrosine residues located within the activation loop.[2] When activated, ERK1/2 phosphorylate several downstream substrates involved in both nuclear and cytoplasmic components[3, 4], leading to a wide range of cellular events including cytoskeletal changes, transcriptional activation, which promote cell cycle progression and also regulate negative feedback mechanisms.[5]

The ERK pathway is aberrant activated in more than 30% of human cancers through a high frequency of genetic alteration. BRAF mutation has been identified in colorectal (10%), thyroid (~ 50%) and melanoma (60%) tumors, whereas RAS is mutated in melanoma (20%), colorectal (50%) and pancreatic (90%) tumors[6], and thus has attracted significant interest as a therapeutic target for cancer. Specifically inhibit BRAF and its downstream effectors MEK have shown promising activities in the clinical to target BRAF and RAS mutant tumors. In particular, the BRAF inhibitors, vemurafenib[7] and dabrafenib[8], and the MEK inhibitor, trametinib[9] and cobimetinib[10] as treatments for BRAF-mutant

metastatic melanoma, validate the strategy of targeting the ERK pathway as an effective way of treating cancer. However, acquired resistance to BRAF inhibitors is often occurs in some patients due to genetic alteration resulting in pathway reactivation[11-14], and limited efficacy as single-agent therapies has been reported with MEK inhibitors[15]. Additionally, negative feedback loops within the ERK pathway lead to pathway reactivation when inhibits single node, driving innate resistance of some RAS and BRAF mutant tumors to BRAF or MEK inhibitors[16]. The emerged resistance to BRAF and MEK inhibitors has led to greater interest in directly targeting ERK, a downstream key signaling node of the MAPK pathway, to provide alternative therapeutic option in tumors with mutations in RAS or BRAF genes and also may have clinical utility in overcoming acquired resistance to BRAF and MEK inhibitors.[17]

In contrast to the advanced development of BRAF and MEK inhibitors, the development of small molecule inhibitors of ERK has fallen behind. Stimulated by the key role of the ERK in MAPK pathway, multiple groups have developed their ERK inhibitors, including several reaching clinical trials (Figure 1), such as GDC-0994 (1)[18], BVD-523 (2)[19], SCH7729984 (3)[20], CC-9003 (4)[21], MK-8353[22], LTT462[23], KO-947[24]. However, the clinical trials involving ERK inhibitors are slow and some have recently been terminated or no longer recruiteparticipants.[21, 23] Therefore, the identification of high-quality inhibitors of ERK1/2 remains of great interest. Herein, we report the structure-based design of a novel scaffold derived from **1** and a series of modifications to the scaffold, led to the discovery of **19i** as high-level potent ERK inhibitors.

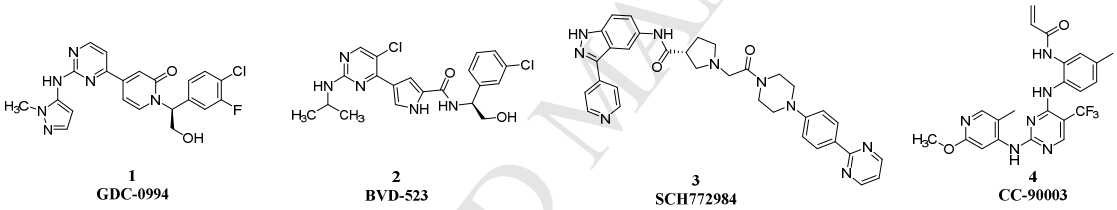

Figure 1. Structures of published clinical ERK1/2 inhibitors

2. RESULTS AND DISCUSSION

2.1. Structure-Based Design of Novel ERK Inhibitors

BVD-523 (Figure 2) is an ATP competitive ERK inhibitor[19], which was chosen as a lead compound in our new structure design. In the docking structure of BVD-523 bond to ERK2 (PDB code 5K4I), the nitrogen of pyrimidine ring accepts one hydrogen bond from the hinge NH of Met108 while the 2-amino group donates one hydrogen bond to the carbonyl oxygen of the same residue. Additionally, the pyrrole-2-carboxamide oxygen makes H-bonds with water mediated H-bond to Gln105 and catalytic Lys54. The 3-chlorophenyl group inserts into a hydrophobic pocket under the glycine-rich loop. The hydroxyl group is forms H-bond from the side chains of Asp167 (Figure 2A). In the aspect of designing a new scaffold, it was desirable to maintain the critical interactions between BVD-523 and the ERK2 protein. We speculated that the pyrrole-2-carboxamide moiety in BVD-523 might be effectively replaced by an isoindolin-1-one linker, as shown in Scheme 1, based on the following considerations. First, modeling studies (Figure 2B) showed that the isoindolin-1-one carbonyl could mimic the oxygen of pyrrole-2-carboxamide, form the same hydrogen bond to Lys54 and water mediated hydrogen bond to Gln105. Second, overlap modeling of the isoindolin-1-one and pyrrole-2-carboxamide scaffold revealed that the left-part pyrimidine formed critical H-bond with hinge and right-part benzyl moieties occupied the same cave under glycine-rich loop (Figure 2B). Thus, we designed and synthesized the isoindolin-1-one derivatives 12a~12l. Considering the hydroxymethyl

group could form H-bonds with Asp167 and Asn154 residues, we also synthesized the isoindolin-1-one derivatives 19a~19l with hydroxymethyl group.

Scheme 1. Structure-Based Design: From 4-pyridone to isoindolin-1-one

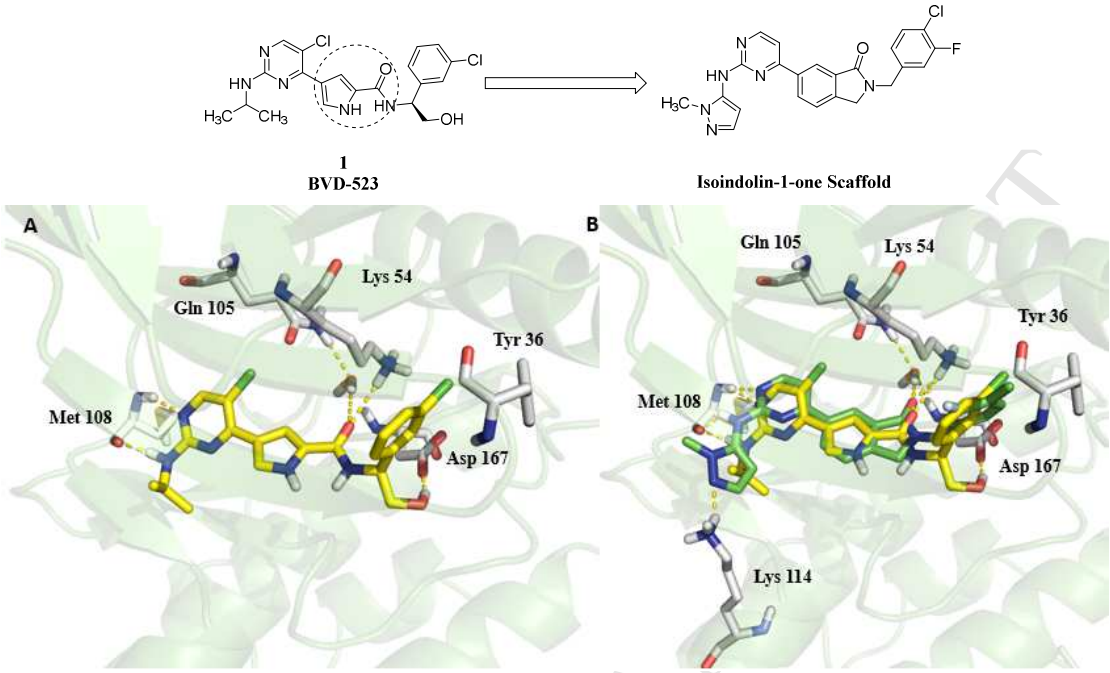

Figure 2. (A) BVD-523 docked into X-ray structure of ERK2 (PDB code 5K4I). Hydrogen bond interactions are illustrated with yellow dashed lines. (B) Overlap of the proposed binding modes of **12a** (green) and BVD-523 (yellow) in ERK2 (PDB code 5K4I). The figure was generated using PyMol (http://www.pymol.org/).

2.2. Chemistry

The isoindolin-1-one derivatives **12a-12l** were synthesized via two different procedures described in Scheme 2 and Scheme 3. In Scheme 2, Pinacol boronate ester **6** was prepared by palladium mediated coupling from compound **5**, followed by protection of amide obtained compound **7**. Then a second palladium catalyzed Suzuki-coupling to furnish the pyrimidine derivative **8** and deprotection to get amide **9**. The N-substituted isoindolin-1-one derivatives **10a-10e** were prepared with sodium hydride and the corresponding benzyl bromide. Later **10a-10e** were oxidized to sulfone **11a-11e**, then displacement of 2-methylsulfonyl group with corresponding amine gave the final compounds **12a, 12b and 12f-12l**. In Scheme 3, Pinacol boronate ester **14** was prepared by palladium mediated coupling from compound **13**. Brominated with **14** gave aryl bromide **15**, which was cyclized with corresponding amine to intermediate **16a-16c**. A palladium catalyzed Suzuki-coupling to furnish the pyrimidine derivative **17a-17c**. Then a second palladium catalyzed Buchwald-coupling with corresponding amine gave compounds **12c-12e**.

Hydroxymethylated analogues **22a-22l** were prepared as illustrated in Scheme 4. Suzuki coupling of **14** and commercially available 4-chloro-2-(methylthio) pyrimidine produced compound **18**, which was converted to the intermediate **19** via oxidation. Brominated with **19** gave aryl bromide **20**, which was cyclized with corresponding benzyl amine to key intermediate **21a-21c**. Installation of the corresponding amine afforded **22a-22l**. Hydroxymethylated analogues such as **24a-24e** requiring a slightly different synthesis route as illustrated in Scheme 5. TBS protected **23** installed the corresponding amine followed by TBS deprotection afforded **24a-24e**. The **(*S*)** or **(*R*)-22i** and **(*S*)** or ***(R)*-22l** were prepared by corresponding (*S*) or (*R*) benzyl amine within scheme 4.

Scheme 2. Preparation of Compounds 12a, 12b and 12f-12l[a]

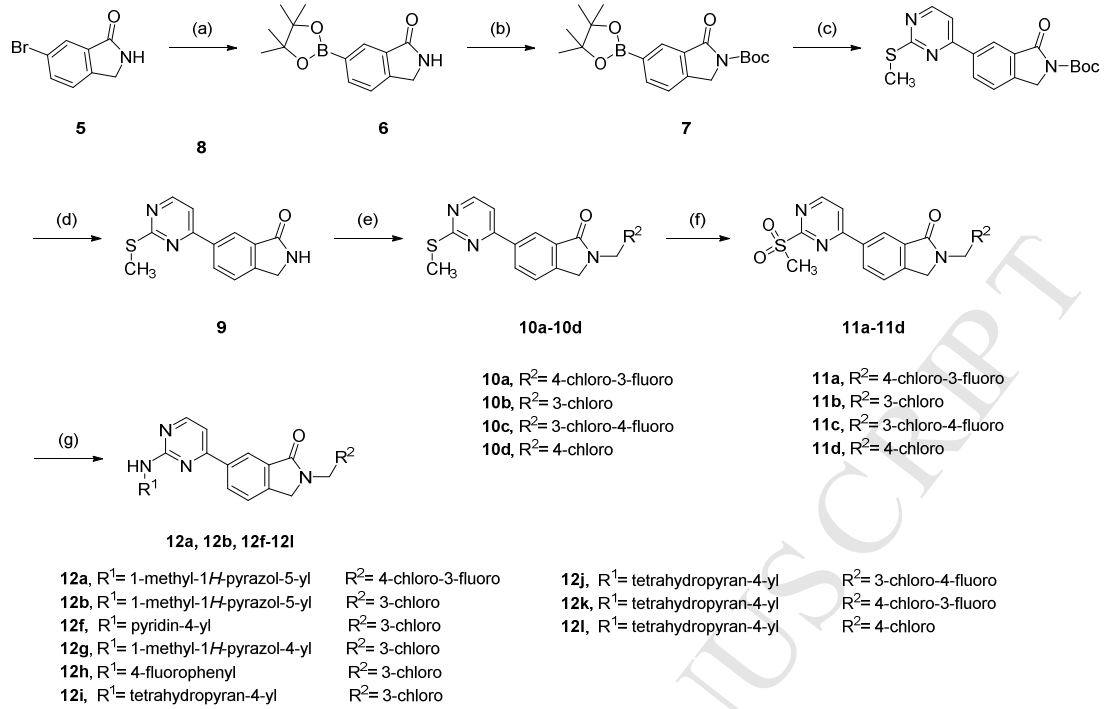

[a]Reaction conditions: (a) $B_2(pin)_2$, KOAc, $Pd(dppf)Cl_2$, dioxane, N_2, 90 °C, 12 h, 71%; (b) $(Boc)_2O$, DMAP, DCM, 25 °C, 2 h, 96%; (c) 4-chloro-2-(methylthio)pyrimidine, $Pd(PPh_3)_4$, Na_2CO_3, PhMe/MeOH/H_2O, 70 °C, 8 h, 90%; (d) TFA, DCM, 25 °C, 1 h, 95%; (e) corresponding arylmethyl bromide， NaH, dioxane, 80 °C, 12 h, 55%; (f) m-CPBA, DCM, 25 °C, 5 h, 83%; (g) corresponding amine, 2-butyl alcohol 125°C, 12 h, 31%.

Scheme 3. Preparation of Compounds 12c-12e[a]

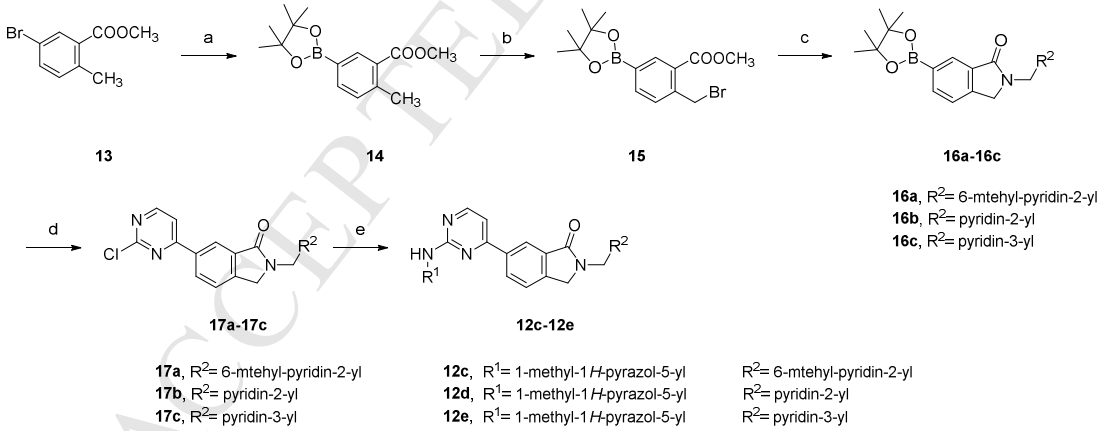

[a]Reaction conditions: (a) $B_2(pin)_2$, KOAc, $Pd(dppf)Cl_2$, dioxane, N_2, 90 °C, 5 h; (b) NBS, BPO, CCl_4, 80 °C, 4 h; (c) 2-Aminomethyl-6-methyl-pyridine or 2-Aminomethyl pyridine or 3-Aminomethyl pyridine, Et_3N, MeCN, 70 °C, 12 h; (d) 2,4-dichloropyrimidine, $Pd(PPh_3)_4$, K_3PO_4, dioxane/H_2O, 80 °C, 12 h; (e) $Pd(OAc)_2$, XantPhos, Cs_2CO_3, 1,4- dioxane, N_2, 100 °C, 12 h.

Scheme 4. Preparation of Compounds 22a-22l[a]

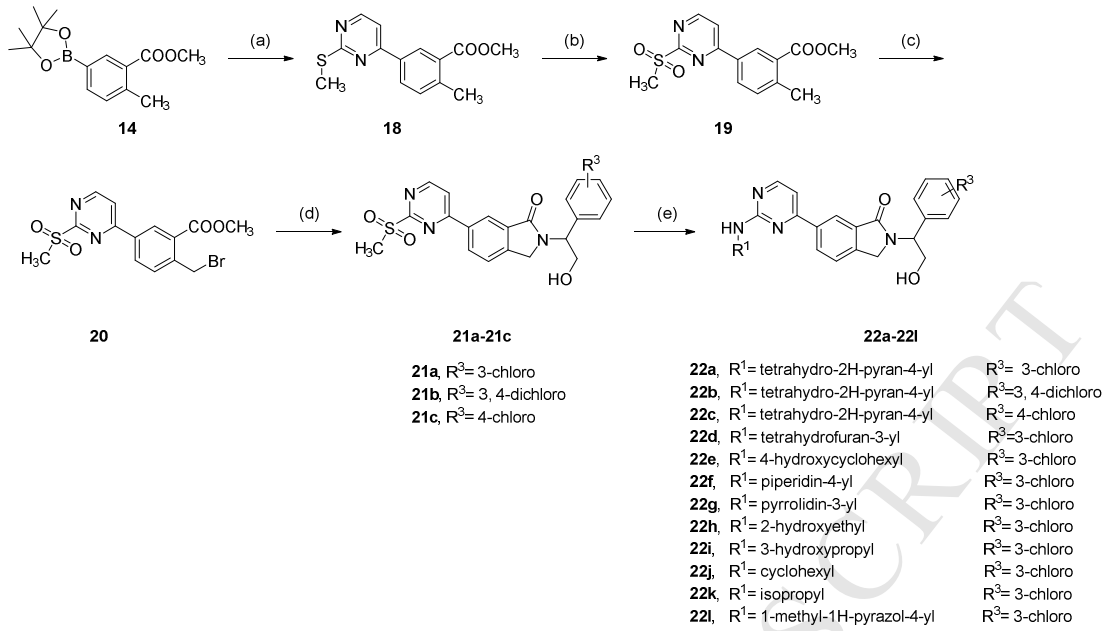

[a]Reaction conditions: (a) 4-chloro-2-(methylthio)pyrimidine, $Pd(PPh_3)_4$, Na_2CO_3, PhMe/MeOH/H_2O, 70 °C, 8 h, 88%; (b) m-CPBA, DCM, 25 °C, 5 h, 95%; (c) NBS, AIBN, Benzene, 80 °C, 4 h; (d) corresponding amine, Et_3N, MeCN, 85 °C, 8 h; (e) corresponding amine, 2-butyl alcohol, 125 °C, 12 h, 33%.

Scheme 5. Preparation of Compounds 24a-24e[a]

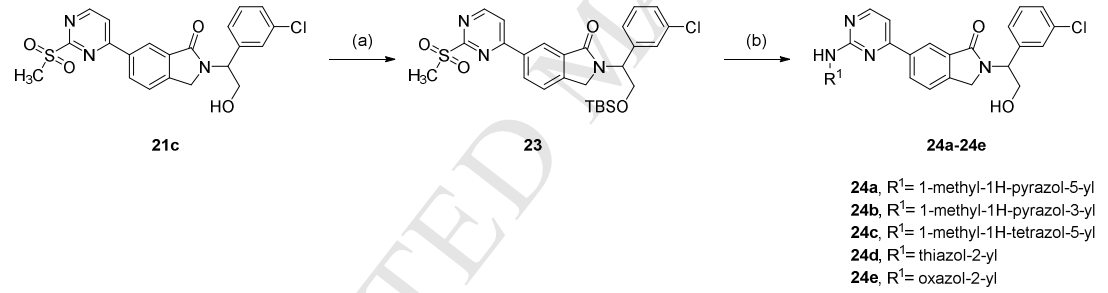

[a]Reaction conditions: (a) TBSCl, imidazole, DCM, 35 °C, 8 h, 95%; (b) corresponding amine, LiHMDS, THF, -78 °C, 3 h, then HCl (gas), 3 h, 20%.

2.3. *In Vitro* ERK Inhibition Assay

To test the hypothesis that isoindolin-1-one scaffold could mimic the pyrrole-2-carboxamide of BVD-523, we first introduced the isoindolin-1-one without considering the hydroxymethyl group in BVD-523. It was found that compound **12a** showed a promising activity with an enzyme IC_{50} = 5.6 nM. This encouraging result confirmed the rationality of our docking experiments and gave us more confidence in using this scaffold to proceed SAR. Thus 1-methyl-1H-pyrazol-5-yl group was employed for our initial SAR studies (Table 1). It is gratifying that the 3-chlorobenzyl analogue **12b** was more potent than **12a**, but other analogues **12c**, **12d**, **12e** which contain a pyridyl group were almost completely loss of potency indicated that pyridyl group was not tolerated at this position. Then we fixed the 3-chlorobenzyl group and studied SAR of R_1 group (Table1). The pyridyl (**12f**), 1-methyl-1H-pyrazol-4-yl (**12g**), 4-fluorophenyl (**12h**) and tetrahydro-2H-pyran-4-yl (**12i**) were used to mimic the hydrogen receptor 1-methyl-1H-pyrazol-5-yl group in **12b**. The results showed that 1-methyl-1H-pyrazol-4-yl derivative **12g** has the same potent as **12b**, however pyridyl derivative **12f** and 4-fluorophenyl derivative **12h** were less potent than **12b**. Gratifyingly, the tetrahydro-2H-pyran-4-yl analogue **12i** displayed twofold increase of potency over **12b**. Following SAR showed the position of

Cl substituent is critical to the potency (**12j**, **12k**, **12l**), 3-Chlorophenyl (**12i**, **12j**) was favored over 4-chlorophenyl (**12k**, **12l**) in enzyme activity.

Table 1. Initial SAR at Right-Part (R^1) and Left-Part Ring (R^2)

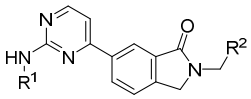

	R^1	R^2	ERK2 IC_{50} (nM)
12a			5.6
12b			3.5
12c			> 1000
12d			> 1000
12e			> 1000
12f			36.3
12g			3.6
12h			> 1000
12i			1.6
12j			2.9
12k			17.8
12l			35.6
BVD-523			0.7

Encouraged by the high inhibitory effect on ERK2 of the novel isoindolin-1-one derivatives with a 3-chlorophenyl at right-part, we then introduced hydroxymethyl group and focused on substituents at left-part (Table 2). First, the hydroxymethyl analogue **22a** resulted in twofold increase in potency over **12i**, indicating the hydroxymethyl group, which could form hydrogen bond with Asp167 and Asn154, is essential to the activity. Second, halogens at the 4- or 3, 4-position (**22b**, **22c**) led to a decrease in potency, which further verified 3-Chlorophenyl was favored over 4-chlorophenyl. Replaced tetrahydro-2H-pyran-4-yl to tetrahydrofuran-3-yl (**22d**) and 4-hydroxycyclohexyl (**22e**) preserve ERK inhibitory potency while replaced oxygen to nitrogen eliminate the enzyme potency (**22f**, **22g**). In addition, the enzyme potency decreased dramatically when the tetrahydro-2H-pyran-4-yl was opened (**22h**, **22i**). The analogues with alkyl substituents such as cyclohexyl and isopropyl groups (**22j**, **22k**) at left-part suffered loss of the enzyme potency. Finally, we explored aromatic groups at left-part. The potency of **22l** and **24a** was maintained over **22a**, while the potency of **24b**-**24e** decreased, presumably due to absence of the interaction with Lys114.

Table 2. Expanded SAR of the Left-Part Ring of Hydroxylated Analogues

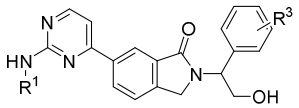

	R^1	R^3	ERK2 IC_{50} (nM)
22a		3-Cl	0.7
22b		3-Cl, 4-Cl	3.1
22c		4-Cl	30.4
22d		3-Cl	5.4
22e		3-Cl	2.7
22f		3-Cl	> 1000
22g		3-Cl	> 1000
22h		3-Cl	17.6
22i		3-Cl	38.4
22j		3-Cl	7.2
22k		3-Cl	11.2
22l		3-Cl	1.2
24a		3-Cl	1.9
24b		3-Cl	25.6
24c		3-Cl	19.8
24d		3-Cl	22.3
24e		3-Cl	93.3

As ERK have two isoforms, in order to completely suppress ERK pathway, we also evaluated part of compounds' ERK1 inhibition activities (table 3). The results showed that our compounds also have good inhibitory effects on ERK1.

Table 3. ERK1 Inhibition Activities of Selected Compounds

	ERK1 IC_{50} (nM)
12g	21
12i	3.3
22a	1.5
22l	4.1
24a	3.6

2.4. Structure-activity relationship (SAR) summary

Based on the results of ERK inhibition screening, we summarized the structure-activity relationship of isoindolin-1-one derivatives (Figure 3). Firstly, the effect of substituent R^1 showed that hydrogen

bond accepter is better than hydrogen bond donor in which tetrahydropyran-4-yl, 1-methyl-1H-pyrazol-5-yl and 1-methyl-1H-pyrazol-4-yl (**12b**, **12g**, **12i**) showed best ERK2 inhibition activities. Secondly, analyzing the effect of R^2 substituents, we found that phenyl > pyridyl and the substitution position at phenyl ring is important for the activity, in which 3-position > 3, 4-position > 4-position (**12i**, **12j**, **12k**, **12l**). Finally, the introduction of hydroxymethyl group at R^3 (**12i** vs **22a**, **12b** vs **24a**, **12g** vs **22l**) further enhanced the activities. Therefore, compounds **12b**, **12g**, **12i**, **22a**, **22l**, **24a** were selected for further studies.

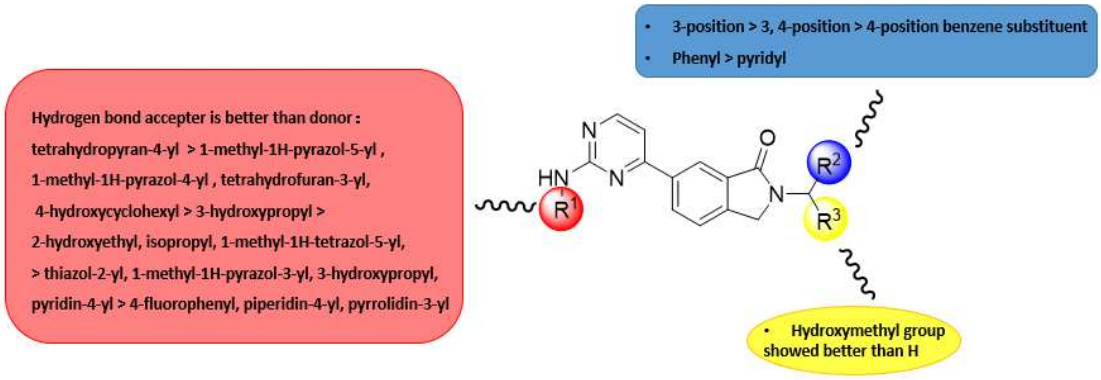

Figure 3. Structure-activity relationship analysis (SAR) of isoindolin-1-one derivatives.

2.5. *In Vitro* Anti-proliferation Assay

Given sufficient potency in inhibiting the intracellular signaling activity of ERK kinase, we then evaluated **12g**, **12i**, **22a**, **22l** and **24a** for their anti-proliferative activities against four tumor cell lines carrying BRAF and K-Ras activating mutations. According to the results in Table 4, all the inhibitors showed moderate activities against Colo205 (BRAFV600E), WM-266-4 (BRAFV600D), SW-626 (KRASG12V) and HCT-116 (K-RasG12D). It was revealed that the IC_{50} of **12g**, **12i** and **22a** against HCT-116 were 148.00±16.27 nM, 150.44±14.16 nM and 154.97±14.16 nM respectively, much higher than other IC_{50} values against tumor cell lines. We also evaluated the anti-proliferation effect of these compounds on K562 cell (Ras & BRAF wild-type). The anti-proliferation activities decreased by more than 10 times which indicated that the effects of these compounds are achieved by affecting the ERK pathway (Table 1 in SI). Western blot analysis was conducted to confirm the intracellular efficacies of **22a**. Result in Figure 4A showed that **22a** could dose-dependent decrease the intracellular phosphorylation levels of ERK1/2 and RSK in HCT116 cells. To determine if apoptosis contributed to the reduced cell proliferation. HCT116 cells were stained with Hoechst 33258 after incubating with **22a** and BVD-523 (Figure 4B). The condensed bright apoptotic nuclei were readily observed. The presence of apoptotic cells was further confirmed by stained with PI and analyzed by flow cytometry (Figure 4C&4D). Hypodiploid DNA appeared in the sub-G0/G1 region, which was represented dead cells.

Table 4. *In Vitro* Anti-Proliferation Activities of Selected Compounds

	IC_{50} (nM)			
	Colo205	WM-266-4	SW-626	HCT-116
12g	203.75±19.27	173.64±17.80	208.84±16.84	148.00±16.27
12i	170.49±15.79	219.89±23.74	254.71±28.47	150.44±14.16
22a	193.53±15.46	259.94±22.34	246.72±26.87	154.97±14.16

22l	226.91±25.46	211.34±17.59	206.12±26.87	200.68±18.48
24a	251.94±25.46	216.57±18.56	252.15±23.97	250.57±24.16
BVD-523	388.81±40.17	230.24±21.39	291.72±31.21	201.74±22.34

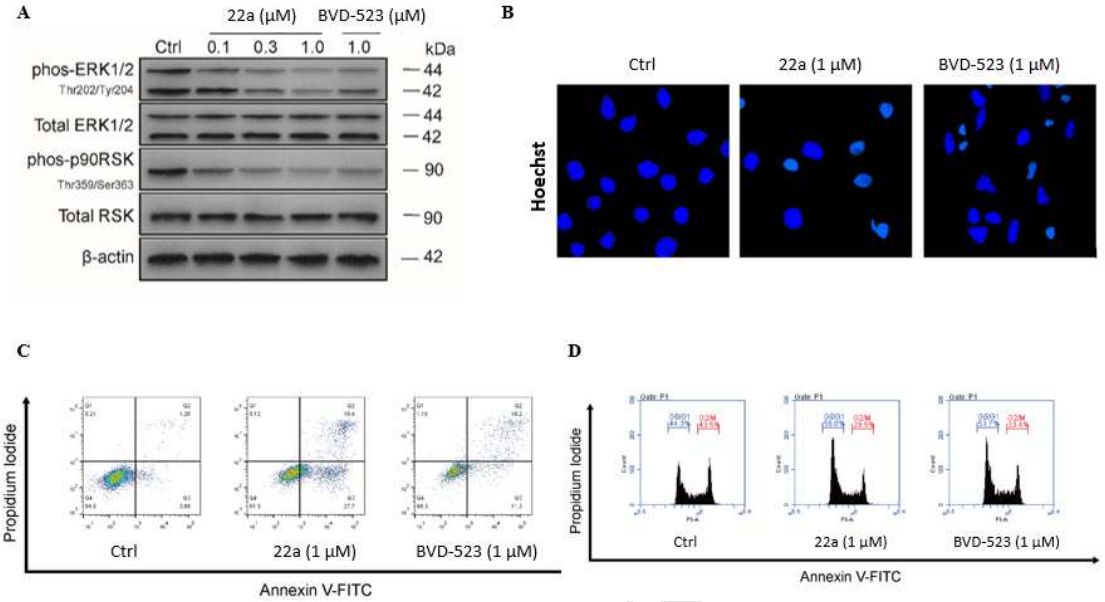

Figure 4. (A) Effects of **22a** on the phosphorylation levels of ERK1/2 and RSK in HCT116 cells. The phosphorylation levels of ERK1/2 and RSK were measured with western blot assay. Results were mean s± SD for three individual experiments which, for each condition, were performed in triplicate. (B) Effects of **22a** on the apoptosis in HCT116 cells. Hochest staining from HCT116 cells in different groups (n=3) (Scale bar: 10 μm). (C) Effects of different **22a** on the apoptosis in HCT116 cells. Cell apoptosis were measured using flow cytometry. Results were means ± SD for three individual experiments which, for each condition, were performed in triplicate. (D) Effects of **22a** on the cell cycle distribution in HCT116 cells. Cell cycle distribution was measured using flow cytometry.

2.6. *In Vitro* Cytotoxic Effects to Normal Cells

It is important to avoid side-effect of new compounds before evaluating *in vivo* activities. Human colonic epithelial cell NCM-460 was chosen to evaluate our compounds' (**22a**, **22l**) cytotoxic effects of normal cells. The result showed that, compounds **22a** and **22l** have no cytotoxic effects at the concentration of 10000 nM, proved our compounds have good safety.

2.7. *In Vivo* Pharmacokinetic (PK) Profile

Compound **12i** and **22a** were selected to investigate in vivo pharmacokinetic characteristics. Two compounds were administrated intravenously (iv) at 5 mg/kg or orally (po) at 50 mg/kg in Sprague-Dawley (SD) rats. The clearance of **12i** (CL = 43.6 mL/min/kg) was higher than **22a** (CL = 23.5 mL/min/kg) at 5 mg/kg (iv). The pharmacokinetic parameters of **12i** and **22a** were respectively shown in Table 5, which indicated that the pharmacokinetic properties of **22a** is superior to that of **12i**. Importantly, **22a** possessed the moderate oral bioavailability (F) of 22.5%, insuring further evaluation of its oral antitumor activity.

Table 5. PK Parameters of 12i and 19a in SD Rats (N = 3)

compd	dose (mk/kg)	$t_{1/2}$ (h)	C_{max} (ng/mL)	AUC_{0-t} (ng·h/mL)	MRT_{0-t} (h)	F (%)

12i hydrochloride	50	0.37	747	1283	1.2	6.9
22a hydrochloride	50	3.6	1920	8380	3.4	22.5

2.8. *In Vivo* Antitumor Activity Evaluation

A HCT-116 xenograft model in nude mice was established to evaluate the in vivo antitumor potency of compound **22a** hydrochloride. **22a** hydrochloride was administered at a dose of 50 mg/kg (po, q.d.) for 30 days, and which could result in 71% tumor growth inhibition (TGI). In comparison, the ERK inhibitor, BVD-523, at a dose of 50 mg/kg (po, q.d.) only resulted in 54% TGI. The tumor growth delay induced by **22a** was visualized by the tumor growth curve in Figure 5A and the final tumor tissue size in Figure 5B. Considering of the potential toxicity of **22a**, we evaluated the nude mice's body weight every 3 days. There was no observed body weight loss with treatment by 30 days in this study (figure 1 in SI), which proved good safety of **22a**.

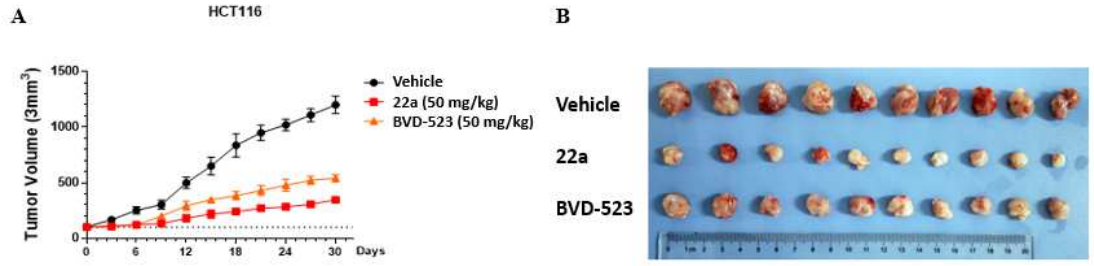

Figure 5. Antitumor efficacy of **22a** in the HCT-116 mouse xenograft model. (A) HCT-116 mouse xenograft data with compound **22a**. (B) The resulting tumors were excised from the indicated groups.

Although racemic **22a** and **22l** possessed good inhibitory effect on ERK2, in order to confirm whether there is difference in ERK2 inhibitory activities between optical isomers, (*S*)-enantiomer and (*R*)-enantiomer of **22a** and **22l** were synthesized using corresponding enantiomer amine (Figure 2 in SI). As anticipated, (*S*)-**22a** and (*S*)-**22l** were 250- and 570-fold more active in the enzyme assay in comparison to (*R*)-**22a** and (*R*)-**22l** (Table 6).

Table 6. SAR of (*S*)-22i, (*R*)-22i, (*S*)-22l, (*R*)-22l

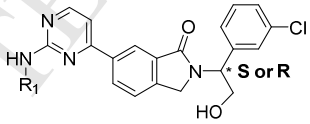

	R_1	Chirality	ERK2 IC_{50} (nM)
(*S*)-22a		*S*	0.8
(*R*)-22a		*R*	201
(*S*)-22l		*S*	1.1
(*R*)-22l	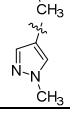	*R*	633

3. CONCLUSION

In summary, a novel series of isoindolin-1-one derivatives targeting ERK was rationally designed, synthesized, and identified. Some of these compounds have excellent biochemical and cellular ERK potencies. Comprehensive and systematic SAR investigation led to the identification of **22a**, a potent and highly efficacious ERK inhibitor. **22a** exhibited excellent ERK inhibitory activities and anti-proliferation potencies. Although **22a** only possessed acceptable pharmacokinetic profiles with the oral bioavailability of 22.5 % in SD rats, but showed considerable activity in vivo antitumor efficacy in a

HCT-116 xenograft model. In addition, **22a** possessed a chiral hydroxymethyl group and further investigation of enantiomer of **22a** showed (*S*)-enantiomer was 250 fold more active in the enzyme assay in comparison to (*R*)-enantiomer (0.8 nM vs 201 nM). Currently, related in vitro and in vivo studies of **22a** enantiomer are in progress.

REFERENCES

(1) Schirmer, A.; Kennedy, J.; Murli, S.; Reid, R.; Santi, D. V. Targeted covalent inactivation of protein kinases by resorcylic acid lactone polyketides. Proc. Natl. Acad. Sci. U.S.A. 2006, 103, 4234−4239.

(2) Dhillon, A. S.; Hagan, S.; Rath, O.; Kolch, W. MAP kinase signaling pathways in cancer. Oncogene 2007, 26, 3279−3290.

(3) Hanahan, D.; Weinberg, R. A. The hallmarks of cancer. Cell 2000, 100, 57−70.

(4) Yoon, S.; Seger, R. The extracellular signal-regulated kinase: multiple substrates regulate diverse cellular functions. Growth Factors 2006, 24, 21−44.

(5) Owens, D. M.; Keyse, S. M. Differential regulation of MAP kinase signalling by dual-specificity protein phosphatases. Oncogene 2007, 26, 3203−3213.

(6) Vakiani, E.; Solit, D. B. KRAS and BRAF: drug targets and predictive biomarkers. J. Pathol. 2011, 223, 219−229.

(7) Flaherty, K. T.; Yasothan, U.; Kirkpatrick, P. Vemurafenib. Nat. Rev. Drug Discovery 2011, 10, 811−812.

(8) Ballantyne, A. D.; Garnock-Jones, K. P. Dabrafenib: first global approval. Drugs 2013, 73, 1367−1376.

(9) Wright, C. J. M.; McCormack, P. L. Trametinib: first global approval. Drugs 2013, 73, 1245−1254.

(10) Garnock-Jones, K. P. Cobimetinib: first global approval. Drugs 2015, 75, 1823−1830.

(11) Montagut, C.; Sharma, S. V.; Shioda, T.; McDermott, U.; Ulman, M.; Ulkus, L. E.; Dias-Santagata, D.; Stubbs, H.; Lee, D. Y.; Singh, A.; Drew, L.; Haber, D. A.; Settleman, J. Elevated CRAF as a potential mechanism of acquired resistance to BRAF inhibition in melanoma. Cancer Res. 2008, 68, 4853−4861.

(12) Wagle, N.; Emery, C.; Berger, M. F.; Davis, M. J.; Sawyer, A.; Pochanard, P.; Kehoe, S. M.; Johannessen, C. M.; Macconaill, L. E.; Hahn, W. C.; Meyerson, M.; Garraway, L. A. Dissecting therapeutic resistance to RAF inhibition in melanoma by tumor genomic profiling. J. Clin. Oncol. 2011, 29, 3085−3096.

(13) Emery, C. M.; Vijayendran, K. G.; Zipser, M. C.; Sawyer, A. M.; Niu, L.; Kim, J. J.; Hatton, C.; Chopra, R.; Oberholzer, P. A.; Karpova, M. B.; MacConaill, L. E.; Zhang, J.; Gray, N. S.; Sellers, W. R.; Dummer, R.; Garraway, L. A. MEK1 mutations confer resistance to MEK and BRAF inhibition. Proc. Natl. Acad. Sci. U.S.A. 2009, 106, 20411−20416.

(14) Poulikakos, P. I.; Persaud, Y.; Janakiraman, M.; Kong, X.; Ng, C.; Moriceau, G.; Shi, H.; Atefi, M.; Titz, B.; Gabay, M. T.; Salton, M.; Dahlman, K. B.; Tadi, M.; Wargo, J. A.; Flaherty, K. T.; Kelley, M. C.; Misteli, T.; Chapman, P. B.; Sosman, J. A.; Graeber, T. G.; Ribas, A.; Lo, R. S.; Rosen, N.; Solit, D. B. RAF inhibitor resistance is mediated by dimerization of aberrantly spliced BRAF(V600E). Nature 2011, 480, 387−390.

(15) Flaherty, K. T.; Robert, C.; Hersey, P.; Nathan, P.; Garbe, C.; Milhem, M.; Demidov, L. V.; Hassel, J. C.; Rutkowski, P.; Mohr, P.; Dummer, R.; Trefzer, U.; Larkin, J. M.; Utikal, J.; Dreno, B.; Nyakas, M.; Middleton, M. R.; Becker, J. C.; Casey, M.; Sherman, L. J.; Wu, F. S.; Ouellet, D.;

Martin, A. M.; Patel, K.; Schadendorf, D. METRIC Study Group Improved survival with MEK inhibition in BRAF-mutated melanoma. N. Engl. J. Med. 2012, 367, 107−114.

(16) Sale, M. J.; Cook, S. J. Intrinsic and acquired resistance to MEK1/2 inhibitors in cancer. Biochem. Soc. Trans. 2014, 42, 776−783.

(17) Hatzivassiliou, G.; Liu, B.; O'Brien, C.; Spoerke, J. M.; Hoeflich, K. P.; Haverty, P. M.; Soriano, R.; Forrest, W. F.; Heldens, S.; Chen, H.; Toy, K.; Ha, C.; Zhou, W.; Song, K.; Friedman, L. S.; Almer, L. C.; Hampton, G. M.; Moffat, J.; Belvin, M.; Lackner, W. R. ERK inhibition overcomes acquired resistance to MEK inhibitors. Mol. Cancer Ther. 2012, 11, 1143−1154.

(18) Blake, J. F.; Burkard, M.; Chan, J.; Chen, H.; Chou, K.-J.; Diaz, D.; Dudley, D. A.; Gaudino, J. J.; Gould, S. E.; Grina, J.; Hunsaker, T.; Liu, L.; Martinson, M.; Moreno, D.; Mueller, L.; Orr, C.; Pacheco, P.; Qin, A.; Rasor, K.; Ren, L.; Robarge, K.; Shahidi-Latham, S.; Stults, J.; Sullivan, F.; Wang, W.; Yin, J.; Zhou, A.; Belvin, M.; Merchant, M.; Moffat, J.; Schwarz, J. B. Discovery of (S)-1-(1-(4-Chloro-3-fluorophenyl)-2-hydroxyethyl)-4-(2-((1-methyl-1H-pyrazol-5-yl)amino)pyrimidin-4-yl)pyridin-2(1H)-one (GDC-0994), an Extracellular Signal-Regulated Kinase 1/2 (ERK1/2) Inhibitor in Early Clinical Development. Journal of Medicinal Chemistry 2016, 59 (12), 5650-5660.

(19) Germann, U.; Furey, B.; Roix, J.; Markland, W.; Hoover, R.; Aronov, A.; Hale, M.; Chen, G.; Martinez-Botella, G.; Alargova, R.; Fan, B.; Sorrell, D.; Meshaw, K.; Shapiro, P.; Wick, M. J.; Benes, C.; Garnett, M.; DeCrescenzo, G.; Namchuk, M.; Saha, S.; Welsch, D. J. Abstract 4693: The Selective ERK Inhibitor BVD-523 is Active in Models of MAPK Pathway-Dependent Cancers, Including Those with Intrinsic and Acquired Drug Resistance. Cancer Research 2015, 75 (15 Supplement), 4693-4693.

(20) Morris, E. J.; Jha, S.; Restaino, C. R.; Dayananth, P.; Zhu, H.; Cooper, A.; Carr, D.; Deng, Y.; Jin, W.; Black, S.; Long, B.; Liu, J.; DiNunzio, E.; Windsor, W.; Zhang, R.; Zhao, S.; Angagaw, M. H.; Pinheiro, E. M.; Desai, J.; Xiao, L.; Shipps, G.; Hruza, A.; Wang, J.; Kelly, J.; Paliwal, S.; Gao, X.; Babu, B. S.; Zhu, L.; Daublain, P.; Zhang, L.; Lutterbach, B. A.; Pelletier, M. R.; Philippar, U.; Siliphaivanh, P.; Witter, D.; Kirschmeier, P.; Bishop, W. R.; Hicklin, D.; Gilliland, D. G.; Jayaraman, L.; Zawel, L.; Fawell, S.; Samatar, A. A. Discovery of a Novel ERK Inhibitor with Activity in Models of Acquired Resistance to BRAF and MEK Inhibitors. Cancer Discovery 2013, 3 (7), 742-750. 27. Chaikuad, A.; M C Tacconi, E.; Zimmer, J.; Liang, Y.; Gray, N. S.; Tarsounas, M.; Knapp, S. A Unique Inhibitor Binding Site in ERK1/2 is Associated with Slow Binding Kinetics. Nat Chem Biol. 2014, 10 (10), 853-860.

(21) Safety and PK Study of CC-90003 in Relapsed/Refractory Solid Tumors. https://clinicaltrials.gov/ct2/show/NCT02313012 (accessed March 9, 2017).

(22) Study of MK-8353 in Combination With Pembrolizumab (MK-3475) in Participants With Advanced Malignancies (MK-8353-013). www.clintrials.gov NCT02972034, April 26th, 2017.

(23) A Phase I Clinical Study With Investigational Compound LTT462 in Adult Patients With Specific Advanced Cancers. www.clintrials.gov NCT02711345, April 26th, 2017.

(24) First-in-Human Study of KO-947 in Non-Hematological Malignancies. www.clintrials.gov NCT03051035, April 26th, 2017.

- 31 novel isoindolin-1-one derivatives were synthesized as ERK inhibitors.
- Antitumor activities of part compounds were evaluated in four cancer cell lines.
- Compound **22a** possesses acceptable pharmacokinetic profiles in SD rat.
- Compound **22a** showed considerable in vivo antitumor efficacy in a HCT-116 xenograft model